Sequential Wavelength Tuning: Dynamics at Interfaces Investigated by Vibrational Sum-Frequency Spectroscopy

SIMON SCHRÖDLE and GERALDINE L. RICHMOND*

Department of Chemistry, University of Oregon, Eugene, Oregon 97403 (S.S., G.L.R.); and Materials Science Institute, University of Oregon, Eugene, Oregon 97403 (G.L.R.)

Vibrational sum-frequency spectroscopy is a powerful tool for the study of interfaces, but its application has hitherto mainly been limited to static structure. This contribution demonstrates how the considerably improved stability of state-of-the-art lasers and parametric generators can be exploited to study the evolution of interfacial structure continuously for several hours. By sequential wavelength tuning and automated control of spatial beam overlap at the target, amplitude changes of sum-frequency resonances in widely spaced infrared regions can be probed. This offers great advantages for the study of the synchronism of molecular processes at interfaces.

Index Headings: **Vibrational sum-frequency spectroscopy; VSFS; Dynamics; Synchronism.**

INTRODUCTION

Vibrational sum-frequency spectroscopy (VSFS) has provided valuable contributions to our knowledge on the structure of interfaces over the last two decades. So far, most investigations have focused on equilibrium states, although it has long been realized that dynamic structures play a key role for many interfacial phenomena.[1] The typical time scale for the equilibration of an interface after a change in bulk composition ranges, depending on the chemistry of the adsorbates and surfaces involved, from a fraction of a second to hours or even days. The principal reason for the lack of dynamic VSFS studies can be found in the prohibitory experimental difficulties: fast phenomena are not easily accessible because of the comparatively high background noise of sum-frequency experiments, which requires prolonged integration periods (averaging), and the investigation of slower processes necessitates stable operation of intricate lasers and parametric generator (OPO/OPA) setups for extended periods of time.

Vibrational sum-frequency spectra can be obtained by two distinctively different experimental approaches that differ by the bandwidth of the infrared (IR) pulses employed. Using a broad-band IR source, all vibrations within a certain frequency range, typically on the order of $\sim$300 cm^{-1}, are excited at the same time and spectra are derived by analyzing the energy distribution of the generated sum-frequency photons. It has been demonstrated that acquisition times of $\sim$30 s for a full spectrum can be realized,[2] which allows data of (relatively slow) kinetics to be accessed. The other common way to perform VSFS measurements is by use of narrow-band IR pulses, whose frequency is scanned to generate a sum-frequency spectrum. Continued refinement of the latter VSFS instruments reported here results in unprecedented improvements of short- and long-term stability. These advances enable the investigation of dynamic processes within a considerable time window.[3–5] Although these studies rely on sum-frequency data at a single frequency only, kinetics can be quantified by monitoring a specific resonance, but information on changes within other regions of sum-frequency spectra is lost. Such data would be valuable for the elucidation of the synchronism of molecular processes at interfaces. While a broad-band approach could resolve this problem by providing full spectra rather than single-frequency data, the bandwidth of broad-band IR pulses is limited in that it does not usually cover a frequency range wide enough to include VSFS signatures that are located in different regions of the IR spectrum, e.g., head group (1000–1600 cm^{-1}) and alkyl chain ($\sim$2900 cm^{-1}) resonances of a surfactant molecule.[2,6] Additionally, from our experience, tuning of the central frequency of broad-band IR pulses often requires manual fine adjustment, and alternating this frequency between two widely spaced values at a sufficiently high rate presents a major experimental challenge. Although these difficulties could be overcome by technical refinement of the instruments, an approach based on a tunable narrow-bandwidth IR beam appears to be more suitable at present.

In this contribution, we show that reliable sum-frequency generation of dynamic processes at interfaces is feasible. An elaborate design allows spatial overlap to be maintained by precise steering of IR and visible (VIS) beams. Such steering is necessary to compensate the inevitable deviations of beam direction and offset caused by the tuning characteristics of the OPO/OPA. With a typical acquisition time for a sum-frequency signal at a single frequency on the order of 5 to 10 s, the VSFS measurements are fast enough to sequentially monitor sum-frequency generation at several wavelengths characteristic for different interfacial species or parts of molecules. This enables us to investigate the synchronism of microscopic processes, and a method is outlined to extract quantitative data, i.e., band amplitudes of VSFS-active transitions and kinetics, from single-frequency VSFS measurements.

EXPERIMENTAL SETUP

The sum-frequency spectrometer comprises a laser, a parametric/difference frequency generator (OPO/OPA/DFG), a beam delivery system controlling spatial and temporal overlap of the VIS and IR beams, the sample holder, and a detection system (Fig. 1). The setup is computer-controlled by LabView Software.

A Nd:YAG laser (PL2143A/SH; EKSPLA, Vilnius, Lithuania) producing 1064 nm and 532 nm radiation was employed as the master light source, emitting $\sim$30 ps pulses at a 10 Hz repetition rate. The tunable IR beam necessary for the VSFS experiments was generated by a PG501/DFG2-10P (EKSPLA, Vilnius, Lithuania) OPO/OPA/DFG setup, which uses β-barium borate (BBO) crystals for parametric generation and a silver thiogallate ($AgGaS_2$) element as the difference-frequency

Received 23 November 2007; accepted 24 January 2008.
* Author to whom correspondence should be sent. E-mail: richmond@uoregon.edu.

0003-7028/08/6204-0389$2.00/0

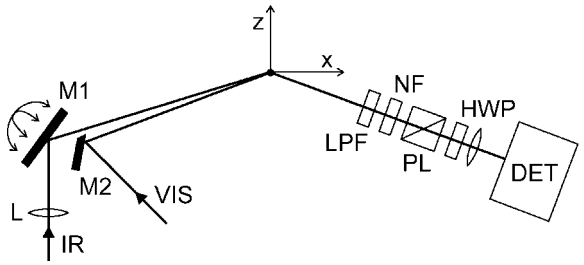

FIG. 1. Schematic view of the sum-frequency experiment (beam generation omitted). The second-order nonlinear polarization of the sample is probed at the origin of the *xyz* frame (*y* axis directed into the drawing plane). IR beam from the DFG stage is focused by lens L and directed to the sample by adjustable mirror M1. Propagation of the VIS beam is controlled by M2. Sum-frequency light is focused on the slit of detector DET after passing through a long-pass filter LPF, a high-attenuation notch filter NF, a polarizer (Glan prism), and a half-wave plate retarder HWP used to optimize the efficiency of DET.

stage. DFG output ranges from 2.3 to 10 μm at a typical pulse energy of 250 μJ in the mid-infrared region.

Tuning of the wavelength is accomplished within ~3 s by angular movements of the nonlinear crystals in the horizontal and vertical plane for the BBO and DFG crystals, respectively. Inevitably, this causes slight frequency-dependent shifts in the position of the emerging IR beam, which are compensated in the vertical plane, where they are most severe, by a steering device before the OPA output reaches the DFG crystal. This compensation is essential not only for an even illumination of the DFG element, but also to maintain spatial overlap at the sample, which is typically located ~1 m from the DFG output. Small additional frequency-dependent walk-off may be introduced by two additional optical elements in the IR beam: a germanium plate employed as a long-pass filter and a barium fluoride (BaF_2) beam splitter, which directs a small percentage of the IR energy to a broad-band IR energy meter. The latter is used, together with a photodiode for the VIS beam, to continuously monitor the beam energies incident on the sample. There, the spot size of the VIS beam is considerably larger than that of the (focused) IR beam and spectral scans over a broad frequency range (e.g., 1350–1600 cm^{-1} or 2800–3800 cm^{-1}) are possible without any additional adjustments. For the current investigations, measurements had to be carried out alternating the IR frequencies over a much wider span because of characteristic VSFS signatures of the adsorbate of interest for our studies located at ~1450 cm^{-1} and 2873 cm^{-1}. This required additional compensation of the variation in IR beam position, implemented using a T-MM motorized mirror mount (Zaber Technologies Inc., Richmond, British Columbia, Canada) with an angular resolution of 1.5 μrad in two axes and a repeatability of <9 μrad. The mirror mount was positioned in the IR beam as shown in Fig. 1 and was also under computer control. From the given geometry it can be derived that the position of the IR beam is reproducibly set to within 18 μm in the x–y plane, an uncertainty deemed reasonably small compared to other possible variations. Calibration of the compensator was performed by maximizing the sum-frequency output at the relevant frequencies (e.g., using the non-resonant VSFS response of a gold surface) preparatory to a series of experiments. With the high level of precision necessary for signal stability and with the inevitable mechanical variations of the whole setup, the calibration settings had to be adjusted approximately every two days.

Note that the slight change of the angle of the reflected sum-frequency beam with IR frequency does not interfere with signal detection because high-efficiency notch filters were employed to suppress residual VIS (and IR) photons rather than narrow spatial filtering (Fig. 1). Furthermore, the active area of the detector (comprising a monochromator, automatically tuned, and a photomultiplier) is large compared to the size and travel of the sum-frequency beam.

SPECTROMETER STABILITY

For the intended experiments, the spectrometer setup has to meet two major criteria. Firstly, parametric generation has to be rapidly tunable between different wavelength settings, even if they are widely spaced, without introducing any significant random errors in pulse energy. Secondly, the beam walk-off compensation mechanism needs to be able to maintain spatial overlap at the sample, because as little as ≈0.05 mm variation of the IR beam position has a measurable effect on the SF signal, even if the IR spot size is considerably smaller than the focus diameter of the VIS beam at the sample.

The reproducibility of IR generation can be easily assessed by inspecting the pulse energy traces continuously recorded during instrument operation. Figures 2a and 2b show typical pulse energy data that were obtained while continuously alternating the OPO/OPA/DFG parameters between the settings for 1453 cm^{-1} and 2873 cm^{-1} frequencies, corresponding to the surfactant head group and alkyl tails, respectively. Short-term fluctuations range from ±1 to 1.5%, depending on the particular wavelength set. Any long-term drift, which mainly originates from changes of the master light source, is not too detrimental for sum-frequency measurements, because all spectral data are generally normalized by the energies of the incident beams. Nevertheless, with the spectrometer well aligned, stable beam generation can be obtained for several hours, with deviations in IR energies hardly exceeding ~3% of their mean values, as shown in Fig. 2c.

We also recorded the intensity of a sum-frequency signal reflected from a gold surface to evaluate the function of the beam walk-off compensator. Metal surfaces show an intense non-resonant signal over the whole IR region, and the power level was kept well below the damage threshold. At the wavelengths used, 1453 cm^{-1} and 2873 cm^{-1}, changes in beam position associated with OPO/OPA/DFG tuning are large enough to severely affect spatial overlap of VIS and IR beams when the frequency is changed. In consequence, only a weak and noisy signal can be recorded if the walk-off compensator setting of the other frequency is used. Sum-frequency traces were normalized by the power of the incident beams and analyzed for noise and residual drift. While a detailed statistical analysis is not provided here and is made difficult by day-to-day variations of laser performance, short- and long-term stability almost reaches the level of experiments performed at a single frequency. Thus, it can be concluded that the implemented wavelength-dependent beam position control is accurate enough and does not introduce any severe additional random errors that would limit the quality of the sum-frequency measurements.

EXEMPLARY APPLICATIONS AND DATA CORRECTION

The instrument and the experimental protocol described above has been used in our laboratory for the investigation of

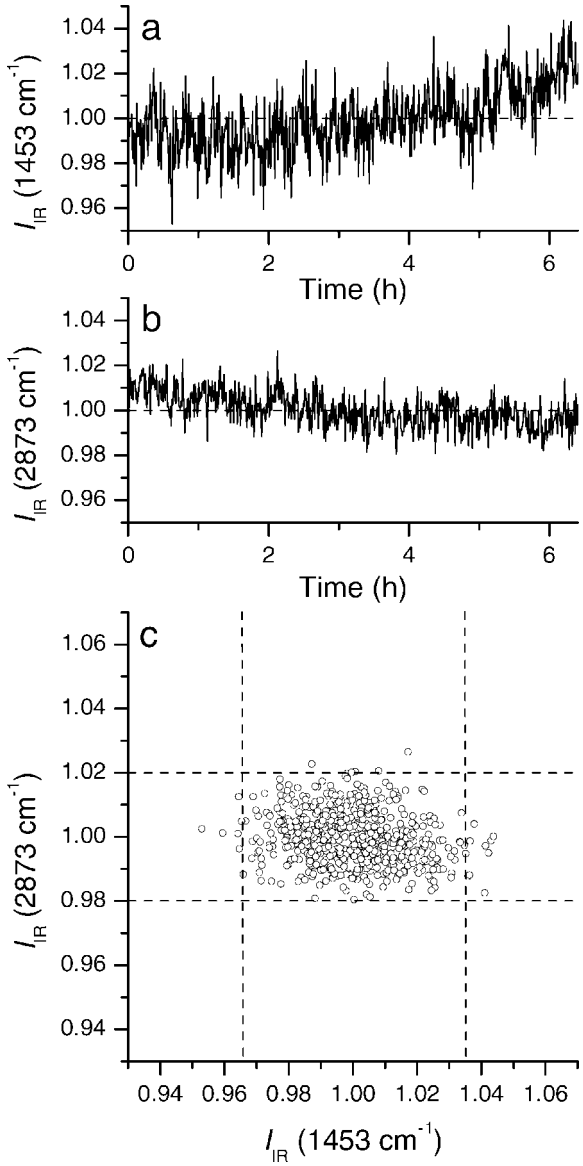

FIG. 2. Long-term stability of DFG output. Parameters of the OPO/OPA and DFG stages were continuously alternated between two wavelength settings, (**a**) 1453 cm^{-1} and (**b**) 2873 cm^{-1} (average pulse energies I_{IR} of 150 shots, normalized by their corresponding mean values, 299 and 465 μJ). (**c**) Correlation plot of both IR energies. Horizontal and vertical dashed lines show ±2% and ±3.5% limits, respectively.

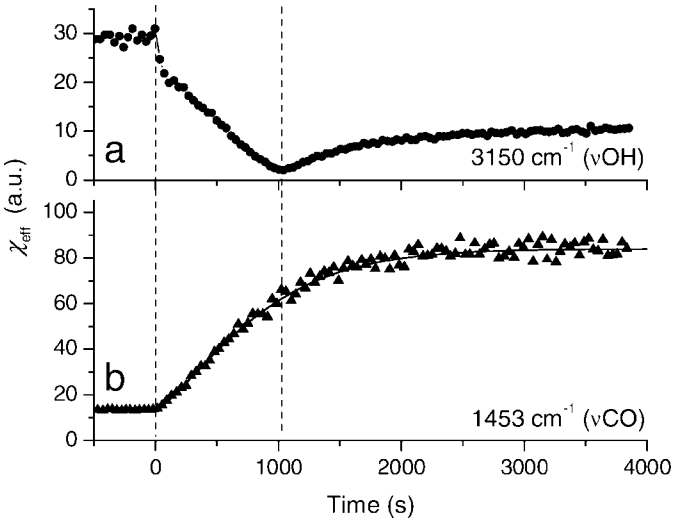

FIG. 3. Adsorption kinetics of sodium dodecanoate (5 μM) at the fluorite–water interface. Effective second-order susceptibilities at (**a**) 3150 cm^{-1} and (**b**) 1453 cm^{-1} as a function of time (in fixed intervals of 39 s).[7]

adsorption, desorption, and equilibrium dynamics of self-assembled monolayers. The chemistry and physics of the underlying processes will be presented in a forthcoming paper,[7] while details of sample geometry and further background information can be found in a recent communication.[8] In the present context, it is important to realize that the adsorbate, dodecanoate (C12), the anion ($CH_3(CH_2)_{10}COO^-$) of a linear carboxylic acid, forms stable monolayers at the fluorite (CaF_2)–water interface, as has been reported for similar carboxylates.[9] The carboxylate head-group of C12 causes a VSFS response at ~1450 cm^{-1} (νCO).[10] Its (hydrophobic) alkyl moiety is made up of methylene (CH_2) groups and a CH_3 terminus. Only the latter is sum-frequency active, because the nonlinear hyperpolarizabilities of the CH_2 groups cancel in the predominant *trans* conformation of the alkyl chains, which are well aligned in the monolayer.[9]

Adsorption of surfactant molecules will disturb the hydrogen-bonding structure at the fluorite–water interface. To investigate the synchronization of changes in the H-bonding structure with the adsorption process, the amplitude of the νOH response of interfacial water molecules was probed by their signal at ~3150 cm^{-1}. Alternating the frequency setting of the instrument, the νCO response was monitored at 1453 cm^{-1}.[7] Figure 3 shows typical data. Individual data points (effective second-order susceptibilities χ_{eff}) represent the square root of the sum-frequency intensity I normalized by the incident IR and VIS energies as an average of 150 laser pulses (15 s sampling time), resulting in a data rate of ~0.05 s^{-1}. Apart from quantitative kinetic information,[7,8] which can be extracted from the individual curves by employing suitable adsorption models, it is directly evident from the drop of the 3150 cm^{-1} signal (Fig. 3) that the number of oriented interfacial water molecules is instantaneously reduced at the start of adsorption ($t = 0$ s, Fig. 3a), while the surface density of surfactant (as measured by the intensity of the carboxylate signal) only slowly rises. At $t \approx 1000$ s, the net orientation of water molecules at the interface vanishes, indicating the point of electrostatic equilibrium. By analyzing the νCO amplitude (1453 cm^{-1}) it can be concluded that adsorption continues well beyond the surface density corresponding to full charge neutralization at the fluorite-aqueous boundary. Equilibrium coverage amounts to nearly ~1.5 times the value at electrostatic equilibrium. Consequently, the interface is then negatively charged, and the water molecules attain an orientation of their dipole vector opposite to that at the neat aqueous CaF_2 interface.[8]

The sequential recording of the traces effectively eliminates systematic deviations arising from the inevitable variations in surface properties of solid, semi-soluble substrates in aqueous environments inherent to an experimental approach using consecutive experiments, each performed at a single frequency.

Unfortunately, recording VSFS intensity at individual frequencies only, rather than determining full spectra, bears some inherent disadvantages if the resonances are narrow-

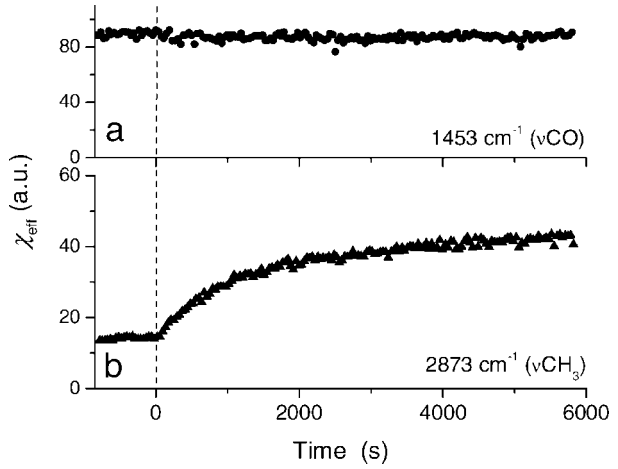

FIG. 4. Monomer exchange kinetics of an equilibrated dodecanoate monolayer at the fluorite–water interface.[8] The exchange process is monitored by alternating the frequencies between (**a**) 1453 cm^{-1} and (**b**) 2873 cm^{-1} to probe the total amount of adsorbed surfactant and the fraction of hydrogenated dodecanoate in the monolayer at a rate of 0.026 s^{-1}.

bandwidth peaks or if they are overlapping with other spectral features. In contrast to linear spectroscopies, VSFS spectra arise from the superposition of (complex) resonant and nonresonant contributions to the second-order susceptibility of the interface.[11] Therefore, constructive or destructive interference of adjacent bands can occur. A nonresonant background signal is also present, and albeit small in the present case, it can be large on metal surfaces.

To cope with these difficulties, a correction method was developed that will be described using an experiment aimed at determining the equilibrium monomer exchange rates of self-assembled monolayers as an example. For these studies,[8] an equilibrated dodecanoate monolayer was prepared from methyl-deuterated surfactant ($CD_3(CH_2)_{10}COONa$). Such monolayers lack any alkyl signals in the 2800–3000 cm^{-1} region but are otherwise identical to their hydrogenated analogues. After recording the VSFS intensities at frequencies characteristic for the νCO and νCH$_3$ resonances (1453 cm^{-1} and 2873 cm^{-1}) over a period of time, the bulk surfactant solution was rapidly exchanged by a solution of the same concentration, but containing only hydrogenated surfactant (at $t = 0$, Fig. 4). The data show that hydrogenated surfactant is incorporated into the monolayer while the total surface density of surfactant (νCO) remains undisturbed.

An inspection of the full spectrum of the resulting monolayer by a numerical fit described elsewhere[12] reveals four resonant contributions (Fig. 5a). Three of them are associated with alkyl resonances, with resonance 2 (Fig. 5a) corresponding to the CH_3 symmetric stretch (resonances 1 and 3 are overtones of bending modes, and 3 is enhanced by Fermi resonance). Contribution 4 is a broad νOH band (with a weak shoulder at higher frequencies[12]). Although the alkyl peaks are sharp and well-defined, there is significant overlap with the νOH band, which causes some changes in signal intensity. Fortunately, all contributions are in phase, i.e., no destructive interference occurs. Such interference could lead to an ambiguous relation between measured band amplitude and surface density. Constructive interference, however, shifts the maximum of the VSFS intensity even when the resonance frequency of the underlying mode is assumed constant. This has been calculated

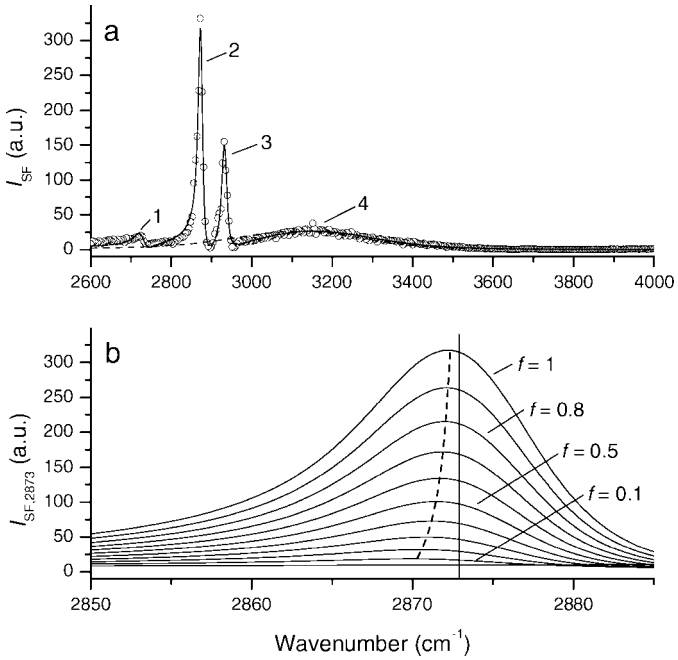

FIG. 5. (**a**) VSFS spectrum of a dodecanoate monolayer on CaF_2. Individual contributions are marked by numbers. Dashed curve indicates contribution 4 only (see text). (**b**) Simulated spectra for CD_3/CH_3 substitution experiment. Fraction of hydrogenated molecules is given by *f*. Vertical line corresponds to 2873 cm^{-1}, dashed curve shows approximate position of the peak maximum (guide to the eye only).

for various mole fractions of hydrogenated surfactant in the monolayer, *f* (Fig. 5b), by systematically changing the intensity of the CH_3 signals in a set of simulated spectra of the interface at full coverage. From these simulated spectra, a correlation can be derived to relate the (measured) nonlinear susceptibility of the surface at 2873 cm^{-1} to the amplitude of the CH_3 resonance. As can be seen in Fig. 6, deviations are most significant at ~20% of the normalized 2873 cm^{-1} signal at fully hydrogenated coverage.

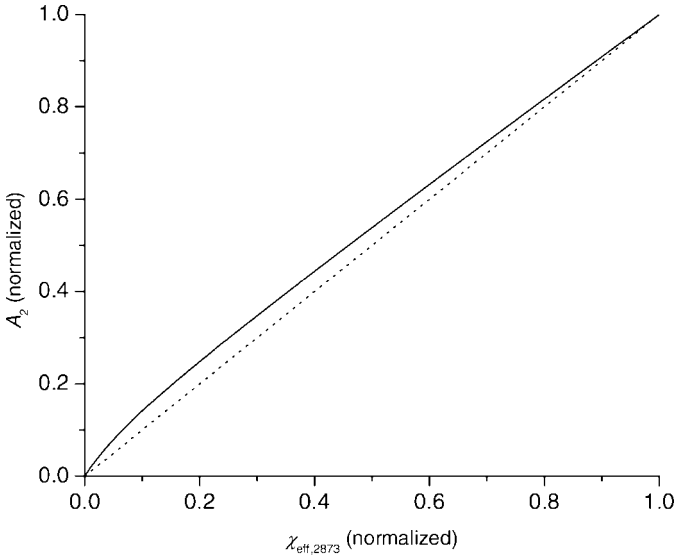

FIG. 6. Relation between band amplitude and effective nonlinear susceptibility at 2873 cm^{-1}, $\chi_{eff,2873}$ as derived from simulated spectra. Dotted line shows linear relationship.

Using the relation of Fig. 6, the composition of dodecanoate monolayers was successfully obtained from the experimental data, thus enabling a quantitative kinetic analysis.[8]

CONCLUSION

This contribution describes the characteristics of a vibrational sum-frequency spectrometer suitable for the investigation of dynamic processes at interfaces within an intermediate time regime (10^2–10^5 s). By controlling spatial overlap and tuning of IR generation to a high level of precision and repeatability, the approach is particularly suitable to investigate the synchronization of interfacial processes. Some first applications of this refined technique are demonstrated, and a way is devised to derive band amplitude and therefore the surface density of individual species from single-frequency measurements.

ACKNOWLEDGMENTS

Financial support for this work was provided by the Department of Energy, Basic Energy Sciences, Grant DEFG02-96ER45557. Equipment provided by the Office of Naval Research is also gratefully acknowledged. S.S. appreciates a scholarship of the German Research Foundation (DFG, Bonn). G.R. acknowledges support for a Fellowship from the Guggenheim Foundation.

1. D. Möbius and R. Miller, *Novel methods to study interfacial layers* (Elsevier, Amsterdam, 2001).
2. G. Ma and H. C. Allen, Langmuir **22,** 11267 (2006).
3. J. Liu and J. C. Conboy, J. Am. Chem. Soc. **126,** 8376 (2004).
4. T. C. Anglin, J. Liu, and J. C. Conboy, Biophys. J. **92,** L01 (2007).
5. M. Smits, M. Sovago, G. W. H. Wurpel, D. Kim, M. Müller, and M. Bonn, J. Phys. Chem. C **111,** 8878 (2007).
6. S. Roke, O. Berg, J. Buitenhuis, A. van Blaaderen, and M. Bonn, Proc. Natl. Acad. Sci. U.S.A. **103,** 13310 (2006).
7. S. Schrödle and G. L. Richmond, J. Am. Chem. Soc., paper in press (2008).
8. S. Schrödle and G. L. Richmond, Chem. Phys. Chem. **8,** 2315 (2007).
9. K. A. Becraft and G. L. Richmond, J. Phys. Chem. B **109,** 5108 (2005).
10. S. Schrödle, F. G. Moore, and G. L. Richmond, J. Phys. Chem. C **111,** 8050 (2007).
11. G. L. Richmond, Chem. Rev. **102,** 2693 (2002).
12. S. Schrödle, F. G. Moore, and G. L. Richmond, J. Phys. Chem. C **111,** 10088 (2007).